JOURNAL OF MATERIALS SCIENCE **40** (2005) 965–972

Characterization of Bi-axial fatigue resistance of polymer plates

H. J. KWON, P.-Y. B. JAR, Z. XIA
Department of Mechanical Engineering, University of Alberta, Edmonton, AB, Canada, T6G 2G8

An approach is proposed to characterize bi-axial fatigue resistance of polymer plates. The method proposed here can detect a change of mechanical properties of polymers (especially ductility) due to fatigue loading, before any visible crack is generated. A decrease in ductility by fatigue loading has been reported for polymers subjected to uni-axial fatigue stresses. Whether a similar phenomenon occurs under bi-axial fatigue stresses is not known at present. In this study, a new bi-axial testing device was designed and built that is capable of applying equal bi-axial forces to cruciform specimens in a cyclic mode. This paper details the test method, including design and instrumentation of the bi-axial testing device, specimen design, and the procedure to determine the load for a desired bi-axial stress state. Poly(acrylonitrile-butadiene-styrene) (ABS) was used as the sample material. Preliminary results reported here show that the ABS's ductility can be reduced significantly by applying 500 cycles of bi-axial fatigue stress at a level that is about 50% of its tensile strength. The results also indicate that such a level of bi-axial fatigue stress has induced extensive rubber particle cavitation, though it is yet to clarify whether the particle cavitation has led to the ductility drop. The study concludes that the methodology proposed in this paper can be used to evaluate bi-axial fatigue resistance of polymer plates for the purpose of materials evaluation.

1. Introduction

The development of fracture mechanics has increasingly influenced design and experimental work involving fatigue life prediction of flawed structural components. It is recognized that in most working structures, stress states in the components are not uni-axial. Biaxial and tri-axial stress states often exist. Unfortunately, standard tests [1, 2] do not provide any information about toughness under multi-axial stress states, as these tests were developed based on linear elastic fracture mechanics that ignores the stresses parallel to the crack growth direction, assuming that they do not have any effect on the fracture behavior or toughness [3, 4]. Furthermore, most of the mathematical and physical models that are being developed in fracture mechanics to rationalize material toughness data are still concentrating on an uni-axial stress environment, and assuming that the transverse stress is secondary and sometimes irrelevant. Since experimental results are yet to clearly support such an assumption, it is not known whether toughness measured in a uni-axial stress state is indeed a proper way to evaluate toughness change of materials under a multi-axial stress state, or whether the crack initiation and growth processes with the presence of transverse stresses are different from those under the uni-axial stress.

Research in the past has investigated mechanical behavior of metallic materials, and showed that in some cases the presence of transverse loading has a significant influence on the mechanical properties. The most well known study that has been mathematically proven by Timoshenko [5] is that the addition of transverse tensile loading increases the critical load for buckling. Other cases that were purely experimental investigations focused on variation of mechanical properties when stress states change from uni-axial to bi-axial. Among these studies, Kelly [6], Hopper and Miller [7], Kitagawa and Yuuki [8], and Hoshide and Tanaka [9] observed that the presence of transverse stress suppressed the damage development, thus increasing the toughness. Work by Joshi and Shewchuk [10] and Hayhurst [11], however, did not support this conclusion. Overall, the presence of transverse stress is believed to increase toughness for metallic materials [12].

For polymeric materials, much fewer studies were conducted. Leevers *et al*. [13, 14] investigated the effect of biaxial loading on resistance to crack growth for poly(methyl-methacrylate) (PMMA) and poly(vinyl chloride) (PVC), and concluded that the effect of transverse tensile stress increases crack resistance for the former but showed little effect on the latter. Atkins *et al*. [15] suggested that the effect of transverse stress is also dependent on the loading mode. The presence of transverse stresses (in other words, in a biaxial stress state) was found to reduce crack growth resistance of poly(acrylonitrile-butadiene-styrene) (ABS) and PVC under monotonic tensile loading, but increased their crack growth resistance under fatigue loading. Since

studies on polymers have been scarce, no general consensus could be reached. At present, it is not clear how the transverse stresses, especially when introduced in a cyclic mode, affect toughness of polymers.

Work described in this paper is to further current understanding of the change of mechanical properties of ABS under biaxial fatigue loading. This is a continuation of previous studies [16, 17] in which the tensile fracture behavior of ABS were found to have been reduced after being subjected to uni-axial fatigue loading. One of the previous studies found that when the fatigue stress was applied at the level equivalent to 50% of ABS's tensile strength, the maximum fracture strain, but not the tensile strength, was greatly reduced. In this paper, the effect of bi-axial fatigue stress on the tensile properties of ABS is reported. An in-house-built test device was used to introduce the bi-axial fatigue loading to specimens which were then fractured under monotonic tension to examine the change of tensile strength and maximum fracture strain (to be named cracking strain in the rest of the text). This paper details the test device, the test methodology, and preliminary results that show how bi-axial loading affects mechanical properties of the ABS.

2. Material

The material used in the study was ABS plate of extrusion grade, with dimensions of 300×300 mm^2 and nominal thickness of 3.2 mm. The plates were prepared by Denki Kagaku Kogyo Co. Ltd., Japan. Rubber particles in the ABS have a bi-modal size distribution, one around 1 μm in diameter and the other 0.1 μm. Preliminary tensile tests showed that the plates are isotropic in mechanical properties, with tensile strength close to 50 MPa and Young's Modulus 2.5 GPa. The ABS contains virtually no gel-like defects. Therefore, using this type of ABS, the possibility of crack initiation from gel-like defects [17, 18] was minimized.

3. Test methodology

The test procedure used in the study is shown in Fig. 1. Firstly, cruciform specimens were machined from the ABS plates, which were then tested under bi-axial fatigue loading at a pre-determined stress level for 500 cycles. After the fatigue loading, dog-bone specimens were machined from the cruciform specimens, and were tested under monotonic tension to measure the tensile strength and cracking strain.

3.1. Specimen design

A cruciform specimen was selected for bi-axial fatigue testing, after consideration of various geometries that in addition to cruciform [19], included tubular [20], inclined crack [15], and rhombic plate [21]. The cruciform design was favored mainly because it allows the application of in-plane biaxial loading without any out-of-plane stress. The crack-free design also allowed us to examine the change of ductility by the fatigue loading. According to our previous study [16], this effect could be quite significant. Overall dimensions of the cruciform specimen are shown in Fig. 2a.

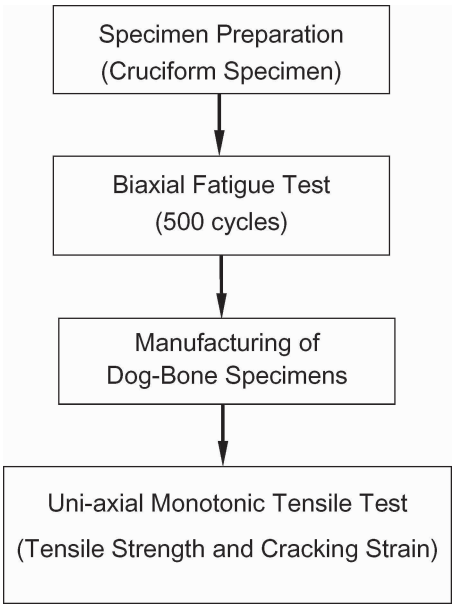

Figure 1 Schematic diagram for the experimental procedure.

It was noted that previous cruciform specimen design, especially those for metallic and fibre composite materials [22, 23], contained thin slots in the four arms to avoid coupling between shear and normal stresses. For ABS, however, the slots were found to contain a significant number of machining defects that induced stress concentration under loading, thus causing premature fracture during the fatigue test. Stress analysis using finite element modeling (FEM), to be detailed later, suggested that for the ABS, coupling between shear and normal stresses is insignificant. Without the slots in the four arms, shear stress in the central part of the cruciform specimen, when subjected to an equal bi-axial loading, was found to be less than 10% of the major principal stress. Therefore, thin slots were deemed unnecessary for the cruciform specimens used in this study.

Some of the cruciform specimens had a thickness reduction in the central square region from 3.2 to 1.28 mm, as shown in Fig. 2b, to raise the bi-axial stress level in the central region. The thickness was reduced gradually, as shown on the cross-sectional view in Fig. 2b, to avoid stress concentration at the ends of the reduced section.

The position of the dog-bone specimens that were machined from each of the cruciform specimens is shown in Fig. 2c. Each cruciform specimen produced 7 dog-bone specimens among which the central 3 specimens had experienced bi-axial stress ratio very close to 1, but the outer four specimens had experienced non-equal bi-axial stresses.

For cruciform specimens of uniform thickness, only the central 3 dog-bone specimens of equal bi-axial stress were used in the following tensile test. For cruciform specimens with reduced thickness in the central region, however, 5 dog-bone specimens were used, of which the central 3 specimens of reduced thickness in the gauge section were subjected to equal bi-axial stress, and the outer-most 2 specimens of the original thickness were subjected to bi-axial stresses at a ratio

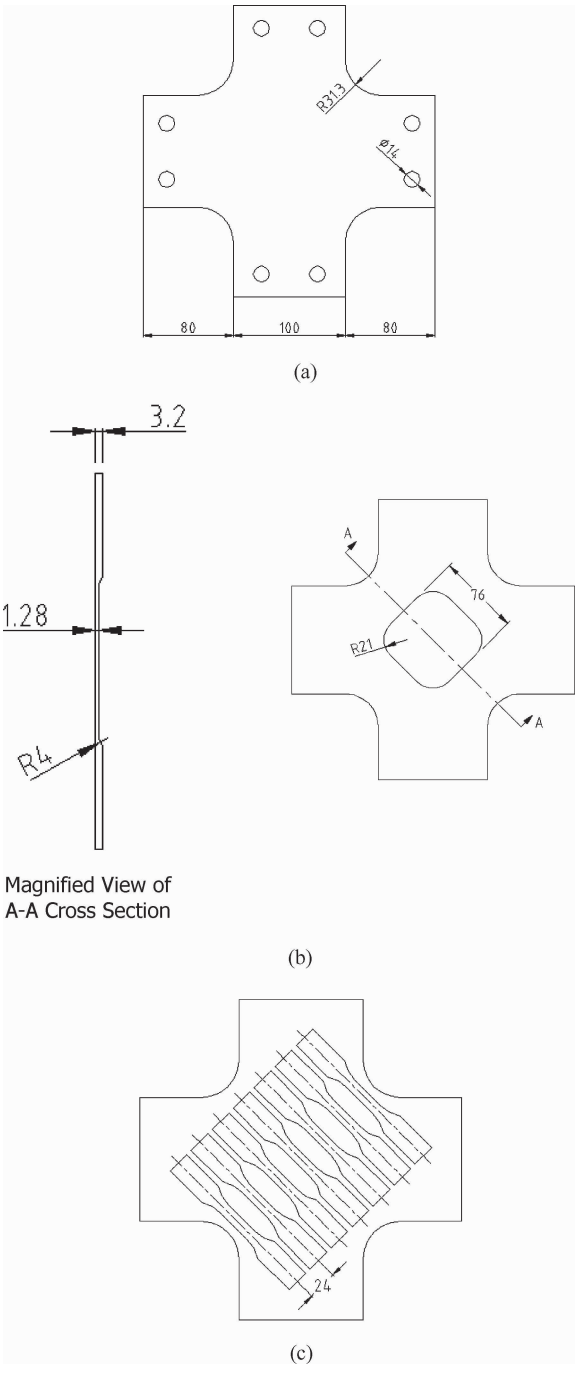

Figure 2 (a) Dimensions of cruciform specimens used for the fatigue loading, (b) dimensions of the central region with reduced thickness, (c) the relative position of 7 dog-bone specimens machined from a cruciform specimen.

of 1:4, with the major stress aligned with the specimen length direction.

Before the testing, corners of the cruciform specimens and edges along the gauge section of the dog-bone specimens were always polished using wet sand papers of 400 and 600 grits to minimize possibility of damage being initiated from the machining-induced defects.

3.2. Finite element analysis

A commercial finite element code, ANSYS R7.0, was used to analyze the bi-axial stress ratio of the cruciform specimens under fatigue loading, in order to quantify the loading history for each dog-bone specimen shown

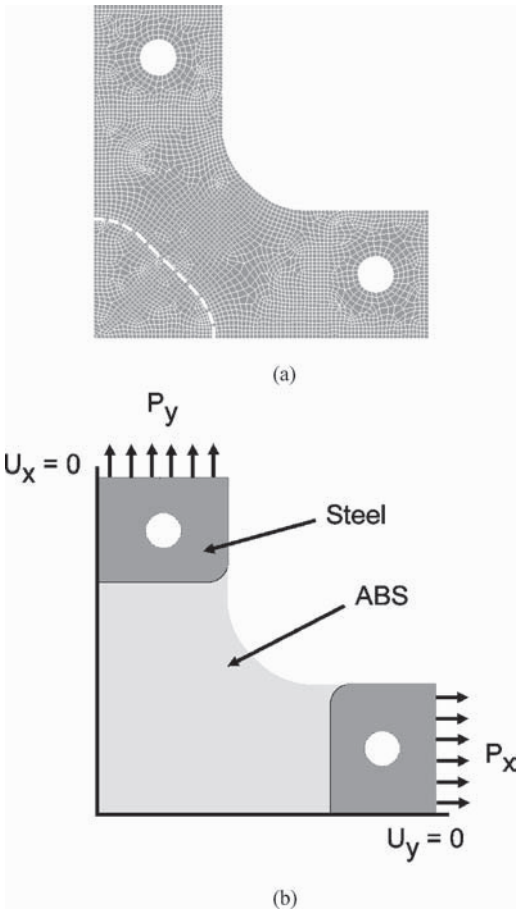

Figure 3 Finite element model: (a) mesh pattern and (b) boundary conditions.

in Fig. 2c, in terms of the fatigue stress level and the bi-axial stress ratio.

A 2-dimensional finite element model was generated to represent one quarter of the cruciform specimen, due to central symmetry of the specimen geometry. The overall model and mesh pattern are presented in Fig. 3a. The elements used were Plane 82, each of which contains 8 nodes. It was assumed that no slippage occurred between the gripper plates and the specimen. Therefore, for the area in the arms that was covered by the gripper plates, Young's modulus (E) was assigned to be that of steel, 207 GPa, and Poisson's ratio (ν) 0.31. For the rest of the model, properties of ABS were used, that is, $E = 2.5$ GPa and $\nu = 0.35$. The thickness of the model was assigned to be the corresponding thickness of the ABS plate. For cruciform specimens with reduced thickness in the central part, the corresponding area in the model, as enclosed by white broken lines in Fig. 3a, was assigned to have a thickness of 1.28 mm.

Boundary conditions of the finite element model are shown in Fig. 3b. Zero normal displacements were assigned along the symmetry lines, i.e., $x = 0$ and $y = 0$, and surface loads, P_x and P_y for loads in x- and y-directions, respectively, were equivalent to the loads applied in the test program.

Fig. 4a shows an example of the stress distribution predicted for a specimen with the original thickness, 3.2 mm. The highest stress level occurs around the corner between the two arms, at a location that is slightly away from point A in the figure. Fig. 4b summarizes

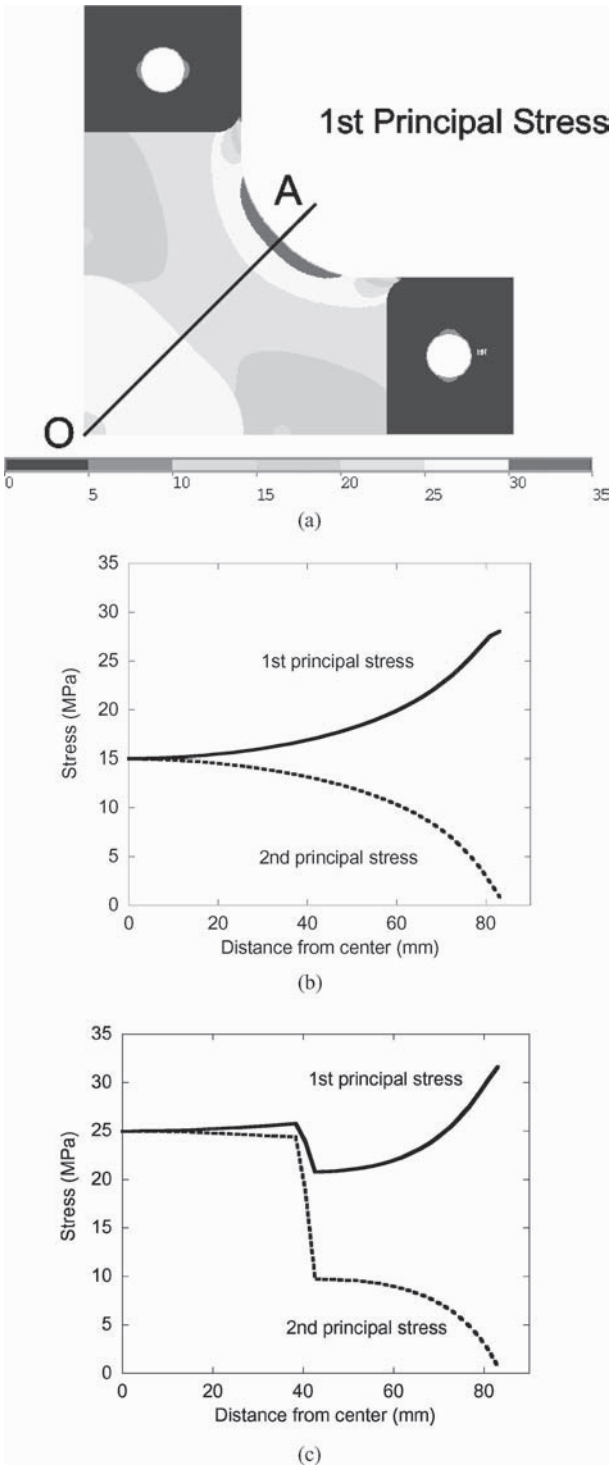

Figure 4 (a) FEM contour plot showing the distribution of the 1st principal stress in the cruciform specimen under equal bi-axial loading, (b) plot of the 1st and 2nd principal stresses along the path OA given in Fig. 4a from specimen with the original thickness, and (c) same as Fig. 4b but from specimen with the reduced thickness of 1.28 mm in the central region.

variation of the 1st and 2nd principal stresses along the diagonal line OA in Fig. 4a. The figure suggests that when the maximum stress around the corner (point A in Fig. 4a) reaches 30 MPa, that was the limiting stress for the ABS subjected to 500 cycles of fatigue loading, the equal bi-axial stress in the central region only reaches a stress level around 15 MPa.

For the cruciform specimens that had the central region reduced from 3.2 to 1.28 mm (40% of the original thickness), the resulting stress distribution along line OA is summarized in Fig. 4c. The figure shows that an equal bi-axial stress of nearly 25 MPa (close to 50% of the tensile strength) is reached in the central region, with much more uniform stress distribution than that shown in Fig. 4b. Although further thickness reduction could raise the bi-axial stress to a higher level, the specimen would have become too fragile to handle. Therefore, the thickness reduction was limited to 1.28 mm.

3.3. Bi-axial test device

Fig. 5a shows the test device for the bi-axial fatigue tests. The device was designed and built in house to fit into MTS hydraulic test frame (Series 812). The base plate of the test device was fixed to the actuating shaft of the MTS machine to generate cyclic vertical motion. Through four connecting rods, the vertical motion was converted to horizontal motion of the sliding blocks that are connected to the grippers to grip 4 arms of the cruciform specimen, as labeled in Fig. 5a. The synchronized horizontal motion of the four grippers applies equal bi-axial cyclic forces to the cruciform specimen. Each of the four sets of sliding block and gripper was mounted on a linear guide rail, linked together through an adjusting bolt that contains a tubular section. Each of the adjusting bolts was screwed into one of the sliding blocks. By turning the adjusting bolt, the distance between the sliding block and the gripper can be changed, which varies the force applied on the four arms of the cruciform specimen.

The tubular section of the adjusting bolt has four strain gauges mounted on the surface to form a full Wheatstone bridge, to measure the force applied in each arm of the cruciform specimen. Therefore, the bi-axial force applied in each arm of the cruciform specimen can

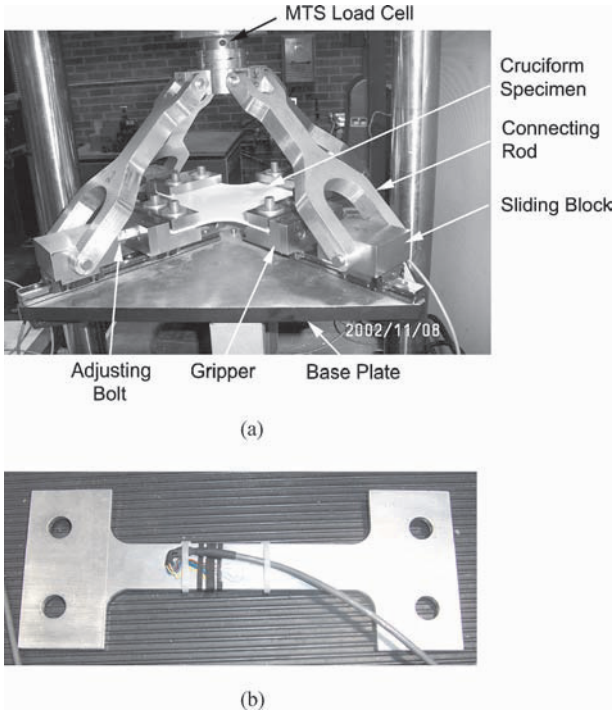

Figure 5 (a) The bi-axial test device and (b) dog-bone calibrator.

be monitored through signals generated by the strain gauges. By turning the adjusting bolts, forces applied in the four arms can be balanced.

Two procedures were devised to calibrate the strain gauge signals. One follows the traditional means of load cell calibration by establishing a master curve of force versus Wheatstone bridge output (in voltage) for each of the adjusting bolts. However, the procedure requires dismantling of the test device, which is tedious and time-consuming, thus impractical to carry out frequently. The other procedure was designed for routine check of the test set-up. It can be carried out by mounting a dog-bone aluminum calibrator, as shown in Fig. 5b, on the fully assembled test device. The calibrator has two strain gauges mounted on the gauge section, and is used to measure forces applied along each axis of the cruciform specimen. This procedure does not provide absolute calibration, but can be used to detect any change of the test set-up. When abnormal signals were detected in this calibration procedure, the test device was then dismantled and each of the adjusting bolts re-calibrated.

In addition to the above two calibration procedures, signals from one of the 4 adjusting bolts are constantly monitored, to ensure that the set-up does not change during the test.

After the cruciform specimen was mounted on the bi-axial test device, and force applied by each of the grippers balanced, signals from the MTS load cell, as shown on the top of Fig. 5a, were used for the fatigue testing in a close-loop, force-controlled mode.

3.4. Bi-axial fatigue test

The total number of cycles for the bi-axial fatigue test was set to be 500. The number was determined based on the previous study [16] in which 500 cycles were found to be sufficient to cause significant reduction of the cracking strain at the fatigue loading level equivalent to 67% of the tensile strength, though the ultimate tensile strength was little affected by the fatigue loading. The stress distribution inside the bi-axial specimen was estimated using the finite element model shown in Fig. 3, i.e. with a given bi-axial stress level in the central region the required force in each arm was determined by finite element model. Then during the test set-up, the specimen was loaded until the force applied in each arm, as measured by the strain gauges, reaches the desired level. The corresponding force read from the MTS load cell was then used as the maximum force for the cyclic fatigue test. The fatigue tests were conducted at a frequency of 0.1 Hz, on loading levels that generated equal bi-axial stresses of 15, 20, and 25 MPa in the central part of the cruciform specimen, which corresponded to 30, 40, and 50% of the ABS's original tensile strength (50 MPa). It should be noted that in this study, cruciform specimens subjected to fatigue stresses of 15 and 20 MPa had the original thickness, but those for 25 MPa had the reduced thickness of 1.28 mm in the central region, in order to raise its stress level relative to that around the corners. In addition, dog-bone specimens that had been subjected to non-equal bi-axial stresses were also examined. As mentioned earlier, these were the outer-most 2 dog-bone specimens in Fig. 2c, under the loading that generated equal bi-axial stress of 25 MPa in the central region.

3.5. Tensile test and microscopic analysis

Tensile tests were used to monitor changes of tensile strength and cracking strain of the dog-bone specimens, in order to correlate the changes with the fatigue loading history. In this study, the tensile tests were conducted using an Instron universal testing machine at a cross-head speed of 5 mm/min. More than 15 dog-bone specimens were used for each bi-axial fatigue loading condition, from which results were averaged and reported here, with scattering bars showing standard deviation among the data points.

A Jeol scanning electron microscope (SEM, model JSM-6301F) was used to examine the fracture surface after the tensile test. Each of the specimens of interest was mounted on a sample holder and then coated with a thin layer of gold just before the SEM examination.

4. Results and discussion

4.1. Mechanical test

Fig. 6 summarizes tensile strength and cracking strain measured from dog-bone specimens after the bi-axial fatigue loading. The horizontal axis is the level of bi-axial fatigue stress experienced by the dog-bone specimens prior to the tensile test. As shown in Fig. 6, tensile strength (○) of the specimens remained constant, having not been affected by the fatigue loading. For the cracking strain after bi-axial fatigue loading, three symbols are used to distinguish the difference in specimen thickness or bi-axial stress ratio. The solid square symbols (■) at 0, 15 and 20 MPa represent data from specimens of original thickness (3.2 mm) with equal bi-axial stresses. The open square symbol (□) at 25 MPa represents data from specimens of reduced thickness (1.28 mm), also subjected to equal bi-axial stresses. The solid triangular symbol (▲) at 30 MPa represents data from specimens of original thickness at a bi-axial stress

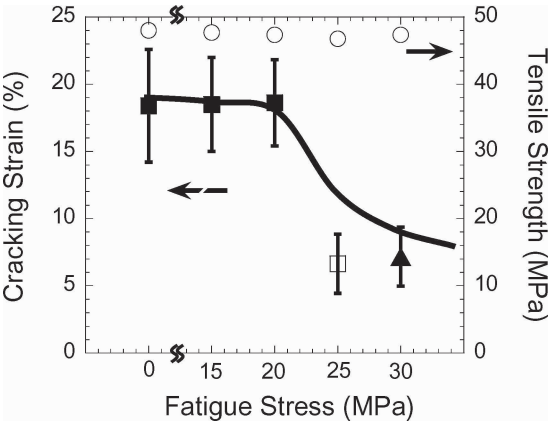

Figure 6 Variation of cracking strain with bi-axial fatigue loading.: ■, from specimens of the original thickness; □, from specimens of the reduced thickness in the central region; and ▲, from specimens subjected to non-equal bi-axial fatigue stresses at a ratio of 1:4. Solid line is the proposed trend of cracking strain variation for specimens of the original thickness.

TABLE I Summary of stress levels and cracking strain values for the ductile-to-brittle transition observed in previous [16] and current studies, using either thick or thin specimens

		Ductile end		Brittle end	
Loading	Specimen thickness (mm)	Stress level (MPa)	Cracking strain (%)	Stress level (MPa)	Cracking strain (%)
Uni-axial fatigue	3.2	15	18	25	5.5
	1.28	–	–	25	2.5
Bi-axial fatigue	3.2	20	18	–	–
	1.28	–	–	25	7

ratio of 1:4, with the major stress (30 MPa) aligned with the specimen length direction. The scattering bars represent standard deviation of the data points each of which, as previously mentioned, was based on results of at least 15 specimens.

Fig. 6 shows that below 20 MPa, cracking strain of the ABS was not affected by 500 cycles of the fatigue loading. A ductile-to-brittle transition, resulting in a significant drop of the cracking strain by almost 65%, occurred when the fatigue stress level increased from 20 to 25 MPa, though the former was applied to specimens of original thickness and the latter to specimens of reduced thickness.

In a previous study of uni-axial fatigue loading [16], a ductile-to-brittle transition, with a drop of around 70% of the cracking strain, was also observed in specimens of original thickness (3.2 mm), but commenced at a lower stress level of 15 MPa, instead of 20 MPa shown in Fig. 6. When specimens of reduced thickness were used at the brittle end of the transition, 25 MPa, the cracking strain was found to be in the vicinity of 2.5%, i.e. reduced by further 16%. Data values from the two types of specimens overlapped at 25 MPa. For clarity, the values are summarized in Table I, which also includes the data from Fig. 6 for comparison. The table suggests that commencement of the ductile-to-brittle transition under uni-axial fatigue loading was 5 MPa lower than that under bi-axial fatigue loading, but the thickness reduction from 3.2 to 1.28 mm did not affect the measured cracking strain values significantly. As suggested in the previous work [16], the increase of surface roughness, caused by the milling process, was believed to be the main cause of the further drop of the cracking strain when the specimen thickness was reduced. Therefore, if specimens of the original thickness were tested under equal bi-axial fatigue loading at 25 MPa, the cracking strain would only be at a similar level as that shown in Fig. 6, probably higher than 7% in value, due to the reduction in surface roughness.

Based on the above discussion, it is believed that ductile-to-brittle transition also exists in ABS when subjected to bi-axial fatigue loading, but the reduction of cracking strain through the ductile-to-brittle transition should be less than that introduced by uni-axial fatigue loading. Further study using specimens of the same thickness and surface roughness is required to verify the conclusion.

A solid line is depicted in Fig. 6 to suggest the trend of the cracking strain variation with respect to the fatigue loading as the stress levels go through the ductile-to-brittle transition of the ABS, if thickness had remained constant, 3.2 mm. The line lies above the open square symbol, to take into account of the cracking strain reduction due to the increase of the surface roughness, caused by the milling process. The solid line also lies slightly above the solid triangular symbol which represents the cracking strain for specimens subjected to bi-axial fatigue loading at a stress ratio of 1:4. Had equal bi-axial stress of 30 MPa been applied to these specimens, based on the conclusion drawn by Atkins *et al*. [15], the cracking strain should have been raised slightly. The solid line predicts that the transition for ABS occurs between 20 and 25 MPa under equal bi-axial fatigue loading.

By comparing the results shown in Fig. 6 with those reported previously [16], the ABS seems to have better resistance to bi-axial fatigue loading than to uni-axial fatigue loading. This is based on two observations: (i) the higher fatigue stress level needed to reduce the cracking strain and (ii) the higher cracking strain level after the ductile-to-brittle transition, when subjected to bi-axial fatigue stresses. These results indicate that the toughness drop of the ABS after biaxial fatigue loading is smaller than that after uni-axial fatigue loading. In other words, the transverse stress increases the fatigue resistance of the ABS.

As discussed in the introduction, two distinctively different conclusions were drawn about the effect of the transverse stress on the toughness of polymers. One suggested that the toughness increases with the application of the transverse loadings, while the other suggested that the effect is adverse. Results from the present study support the former conclusion.

4.2. Microscopic analysis

Fig. 7 shows micrographs of fracture surfaces formed in specimens that had been subjected to equal bi-axial fatigue loading of 20 and 25 MPa, and then fractured under monotonic tension. Figs 7a and c were taken from regions that were initiated from fatigue loading, but the fracture surface was actually formed during the tensile test, according to a model proposed in a previous report [16]. Characteristic feature in this region is the relatively smooth surface topography, with many debonded small rubber particles (of around 0.1 μm in diameter) and cavitated or cleaved large rubber particles (of around 1 μm in diameter). Fig. 7c clearly shows more cavitated rubber particles than Fig. 7a, suggesting that the increase of bi-axial stress from 20 to 25 MPa has promoted particle cavitation. The same trend can also be seen for debonding of small rubber particles in these two micrographs.

The above conclusion is also supported by micrographs taken from regions formed by unstable crack growth, as shown in Fig. 7b and d. It is apparent that the surface shown in Fig. 7d has been under more deformation than that shown in Fig. 7b, both of which show extensive deformation around cavities. Since rubber particle cavitation promotes matrix deformation during fracture, cavitation in Fig. 7d should have been more extensive than that in Fig. 7b. It should be noted that

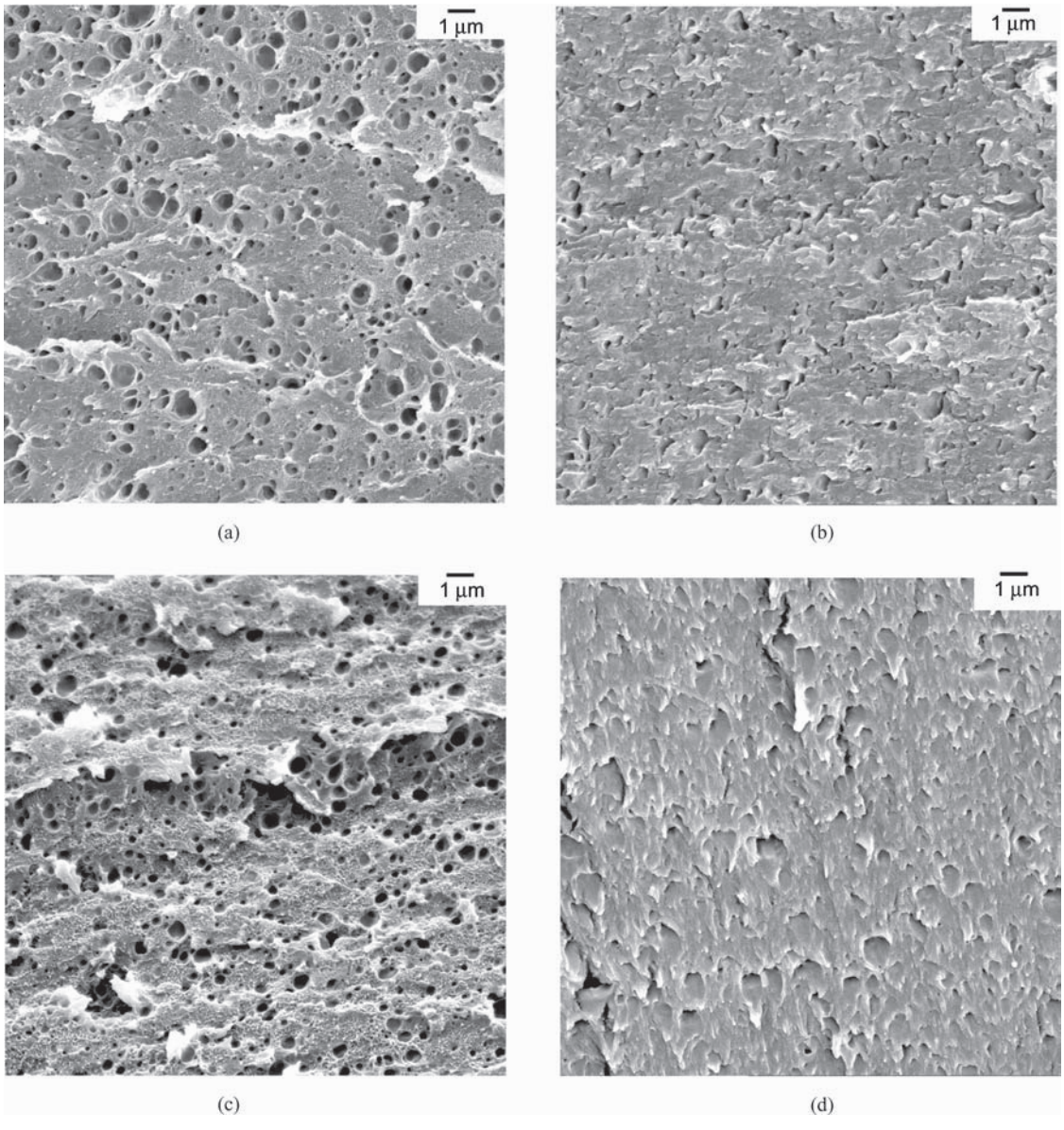

Figure 7 SEM micrographs: (a) from a specimen subjected to equal bi-axial fatigue stress of 20 MPa, in the damage initiation region, (b) from the same specimen as that for Fig. 7a but in an unstable crack growth region, (c) from a specimen subjected to equal bi-axial fatigue stress of 25 MPa, in a damage initiation region, and (d) from the same specimen as that for Fig. 7c but in an unstable crack growth region.

fracture surface formed by unstable crack growth, but not having been subjected to fatigue loading, did not show this kind of surface topography [16]. Therefore, the cavities must have been generated during the fatigue loading. At this stage, however, it is not clear whether the particle cavitation is the direct cause of the drop of cracking strain shown in Fig. 6.

5. Conclusions

A new bi-axial test device was designed and manufactured to introduce bi-axial fatigue loading to plate specimens. Using ABS as a sample material, this paper details design and instrumentation of the bi-axial test device, and proposes an approach that can characterize change of mechanical properties by the bi-axial fatigue loading. By reducing thickness of the central part of the plate specimen, equal bi-axial stress level can be raised. In this study, the bi-axial stress was raised to a level that is close to 50% of the tensile strength of the ABS plate.

Using the device and the test methodology, preliminary results were obtained on how bi-axial fatigue loading affects mechanical properties of the ABS. The results showed a significant reduction of cracking strain when the equal bi-axial stress was increased from 20 to 25 MPa, although the tensile strength did not show any changes. As the specimen thickness used in this study was not kept constant, we could not firmly conclude that the drop of cracking strain is an indication of the ductile-to-brittle transition that was observed when the material was subjected to uni-axial fatigue loading. Nevertheless, the results suggest that the device and the test methodology can be used to study change of mechanical properties of polymers after being subjected to bi-axial fatigue loading.

The study also discovered that by introducing a bi-axial fatigue stress at a level that is equivalent to 50% of the tensile strength of ABS, cavitation could occur in a significant proportion of the rubber particle population. Therefore, the device can potentially be used

to study the effect of particle cavitation on mechanical properties of rubber-toughened polymers, which has long been interesting to researchers but could not be properly investigated.

Acknowledgement

This work was sponsored by Natural Sciences and Engineering Research Council of Canada (NSERC). We are grateful to B. Faulkner and A. Yuen in the Department of Mechanical Engineering, University of Alberta for the technical assistance in mechanical testing, D. Raboud D. Pape for contribution to the early work in instrument design, K. Poorhaydari for assistance in the instrument design and D. Lee in Department of Earth and Atmospheric Science for the SEM examination. Information provided by K. W. Neale in University of Sherbrooke on design of the bi-axial tester and the cruciform specimen is also greatly appreciated.

References

1. J. G. WILLIAMS, in "Fracture Mechanics of Polymers" (Ellis Horwood, Chichester, England, 1984).
2. R. W. HERTZBERG and A. MANSON, in "Fatigue of Engineering Plastics" (Academic Press, New York, 1980).
3. H. M. WESTERGAARD, *J. Appl. Mech.* **6** (1939) 49.
4. P. C. PARIS and G. C. SIH, *ASTM STP* **381** (1964) 30.
5. S. P. TIMOSENKO and J. M. GERE, in "Theory of Elastic Stability" (McGrawHill, New York, 1961) p. 357.
6. D. A. KELLY, *J. Strain Anal.* **11** (1976) 1.
7. C. D. HOPPER and K. J. MILLER, *ibid.* **12** (1977) 23.
8. H. KITAGAWA, R. YUUKI and K. TOHGO, *Fatig. Eng. Mater. & Struct.* **2** (1979) 195.
9. T. HOSHIDE and K. TANAKA, *ibid.* **4** (1981) 355.
10. S. R. JOSHI and J. SHEWCHUK, *Exper. Mech.* **10** (1970) 529.
11. D. R. HAYHURST, *J. Strain Anal.* **8** (1973) 119.
12. E. W. SMITH and K. J. PASCOE, *Fatig. Eng. Mater. & Struct.* **6** (1983) 201.
13. P. S. LEEVERS, J. C. RADON and L. E. CULVER, *Polym.* **17** (1976) 627.
14. P. S. LEEVERS, L. E. CULVER and J. C. RADON, *Eng. Fract. Mech.* **11** (1979) 487.
15. A. G. ATKINS, G. JERONIMIDIS and S. ARNDT, *J. Mater. Sci.* **33** (1998) 4349.
16. H. J. KWON, P.-Y. B. JAR and Z. XIA, *ibid.* **39** (2004) 4821.
17. P.-Y. B. JAR, K. KONISHI and T. SHINMURA, *ibid.* **37** (2002) 4521.
18. R. MARISSEN, D. SCHUDY, A. V. J. M. KEMP, S. M. H. COOLEN and W. G. DUIJZINGS, *ibid.* **36** (2001) 4167.
19. A. A. LEBEDEV and N. R. MUZYKA, *Strength of Mater.* **30** (1998) 243.
20. R. S. KODY and A. J. LESSER, *Polym. Comp.* **20** (1999) 250.
21. S. Y. ZAMRIK and D. C. DAVIS, *ASTM STP* **1191** (1993) 204.
22. A. MAKINDE, L. THIBODEAU and K. W. NEALE, *Exper. Mech.* **32** (1992) 138.
23. Y. YOUSSEF, S. LABONTE, C. ROY and D. LEFEBVRE, *Sci. & Eng. Comp. Mater.* **3** (1994) 259.

Received 28 January
and accepted 31 August 2004